Lateral Track Stability: Theory and Practice in Japan

SHIGERU MIURA

In Japan theoretical and experimental studies have been conducted since the early 1930s to work out effective measures to maintain lateral track stability. In 1957 the theory of track buckling based on the principle of virtual work was established, which is the basis for current practical measures to ensure lateral track stability. The theory defines the minimum buckling strength, which corresponds to the minimum longitudinal load at which a stable distortion wave can exist. Based on the theory and practical experience, laying and maintenance standards for continuous welded rail (CWR) and joint-gap control methods have so far been established, both of which have effectively contributed to lateral track stability. Recently, it has become necessary to use CWR even on sharp curves and to remove expansion joints in front of and behind a turnout to reduce maintenance. From this point of view, it is important to make clear the cause of track buckling and to understand more clearly the behavior of long welded rail connected to turnouts. The historical background and the current status of the theory and practice of lateral track stability in Japan are described in this paper.

Thermal longitudinal forces caused by an increase in the temperature of railway track can cause the track to be laterally and suddenly deformed. This phenomenon, called buckling, is sometimes fatal. Its prevention has been a serious concern of track engineers for a long time, especially with the increased use of continous welded rail (CWR), which has been brought into practical use since the 1950s.

In Japan the first theory of track buckling was presented in 1932. In 1957 the theory of buckling was established and is the basis for various measures currently taken to ensure lateral track stability.

The theoretical basis of CWR was defined in 1934, and in 1937 a 4.2-km-long CWR was laid in a tunnel on a trial basis. Thereafter, through experimental verification, regular laying of CWR was started in 1953. By the end of 1983, when the Japanese National Railways (JNR) was still in existence, the total length of CWR laid was about 7940 km, of which 3470 km is on the Shinkansen lines and 4470 km is on the narrow-gage lines and accounts for about 16 percent of the whole length of those lines.

On the basis of theoretical analyses and practical experience on the buckling stability of track, laying and maintenance standards for CWR and a joint-gap control method have been established in Japan, both of which have been effective contributors to the prevention of track buckling. The theory and practice of lateral track stability of the now-defunct JNR and the Japan Railways (JR) Group, which took over after privatization of JNR, will be described here.

Track and Structure Laboratory, Railway Technical Research Institute, 2-8-38 Hikari-cho, Kokubunji-shi, Tokyo 185 Japan.

THEORY OF LATERAL TRACK STABILITY

Minimum Buckling Strength

It was not until 1932 that studies on lateral track stability were undertaken in Japan. Horikoshi had carried out buckling tests on a full-scale test track fixed with concrete blocks at both ends of a 48-m-long track. In 1934, on the basis of the test results, he established a theoretical equation for track buckling. Around the same time, Inada of Kyushu Imperial University studied railway track buckling as a part of the stability theory of a long column subjected to lateral elastic resistance. Further, in 1938 Hoshino established an expansion and contraction theory of CWR on the basis of expansion tests on a full-scale track and its theoretical consideration. In 1943 Ono derived buckling loads from a differential equation in which the ballast resistance was assumed constant and the balance of a longitudinal rail force in front of and behind a buckling waveform was taken into consideration.

Thereafter, Numata suggested a new buckling theory (*1*) based on the principle of virtual work. This theory is a foundation for the various countermeasures currently taken in Japan against track buckling and is outlined as follows.

The shapes of CWR that are subjected to longitudinal force and laterally buckled are categorized as shown in Figure 1 and approximated with a sinusoidal waveform. Meanwhile, ballast resistance should be constant regardless of displacement, as shown in Figure 2c. Here, the following energies accumulated in a track are taken into consideration:

(a) Strain energy generated by longitudinal force change,
(b) Strain energy generated by rail bend, and
(c) Internal energy created by ballast resistance.

An application of the principle of virtual work to these energies yields the following expression of buckling strength:

$$P_t = P + \left\{\frac{\gamma^2 r^2}{P} + \frac{\alpha r}{P^3 (P)^{1/2}}\left[\left(g - \xi\frac{P}{R}\right)^2 + \kappa\left(g - \xi\frac{P}{R}\right)\frac{P}{R}\right]\right\}^{1/2} - \frac{\gamma r}{(P)^{1/2}} \quad (1)$$

where

P_t = buckling strength,
P = longitudinal rail force balanced after buckling,
g = longitudinal ballast resistance,
r = lateral ballast resistance,

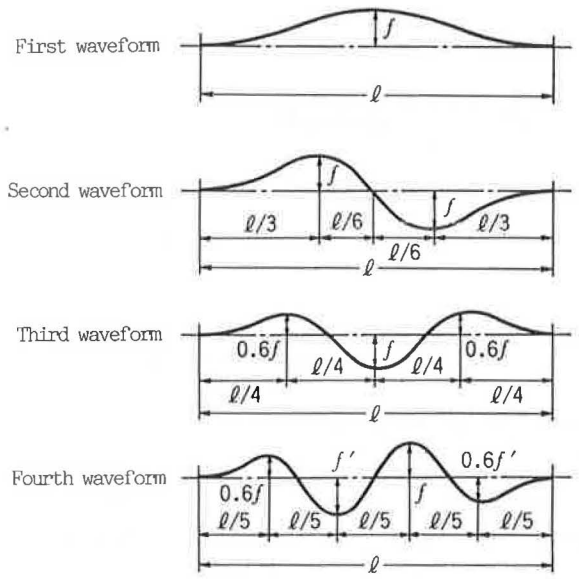

FIGURE 1 Classification of buckling waveforms.

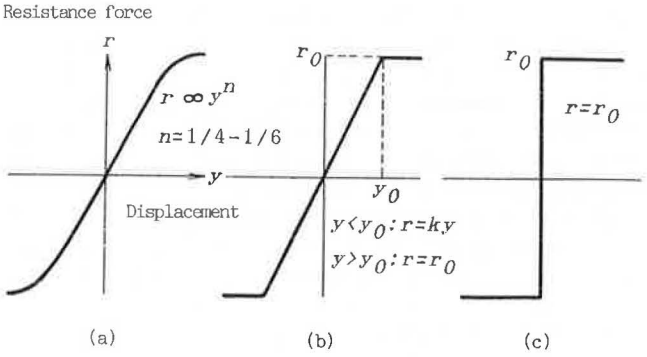

FIGURE 2 Relation between tie displacement and ballast resistance.

R = radius of track curvature, and
$\gamma, \alpha, \xi, \kappa$ = constants that depend on track structures and waveforms.

As for virtual wavelength (l) and displacement (f), the buckling strength determined by the above equation and the relationship between l and f in balance after buckling are shown in Figure 3. The longitudinal force less than the minimum value of buckling strength, as shown by Equation 1 and Figure 3, does not generate buckling.

When minimum buckling strengths by radii of curvature are determined for the various waveforms shown in Figure 1, on tangent track and track with a larger radius of curvature the minimum buckling strength of the second waveform is the smallest, whereas on the track with a smaller radius of curvature the minimum buckling strength of the first waveform is the smallest. The minimum buckling strengths determined for various ballast resistances are shown in Figure 4.

The minimum buckling strength shown in Figure 4 sets a limit at which the longitudinal force less than the one corresponding to the minimum buckling strength cannot bring

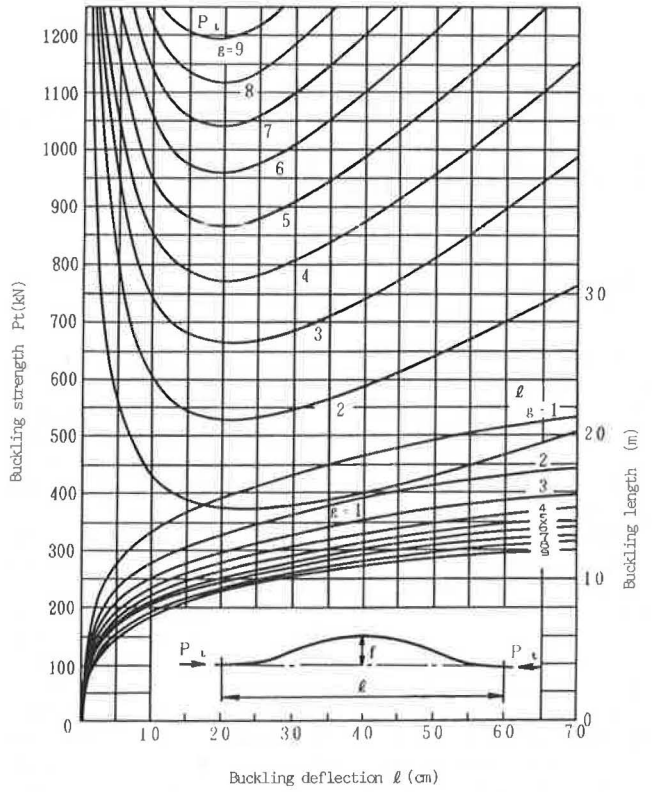

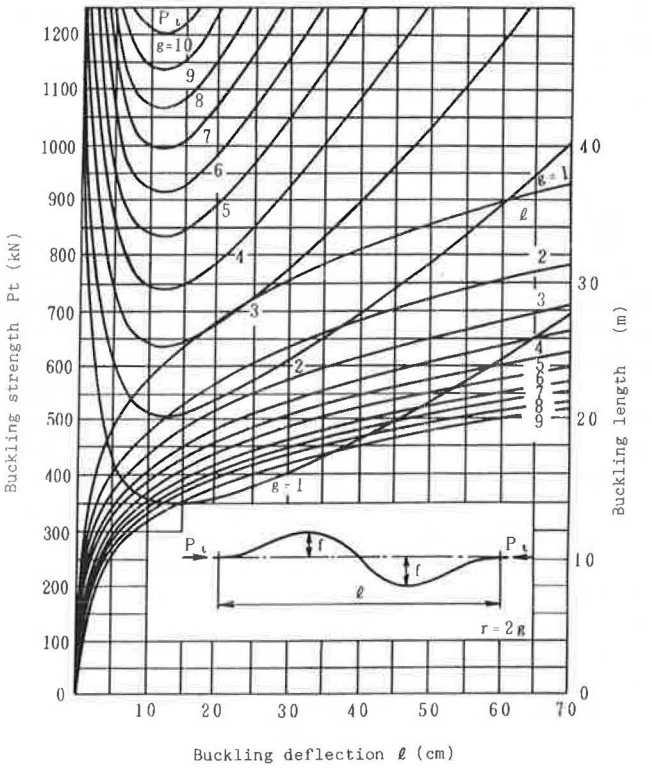

FIGURE 3 Buckling strength of track.

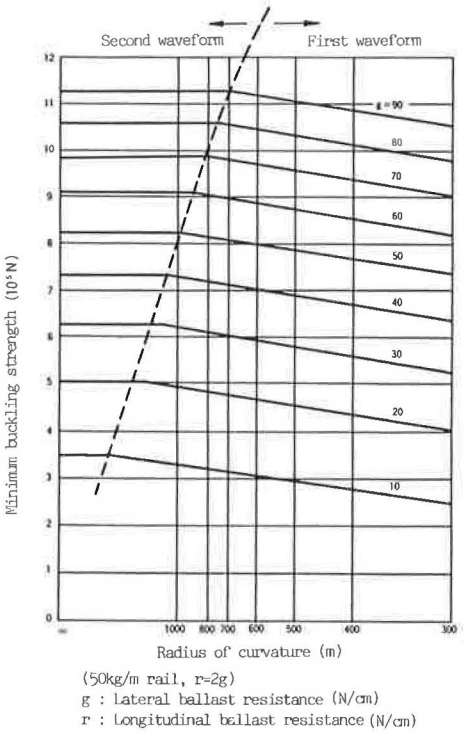

FIGURE 4 Minimum buckling strength as a function of radius of curvature.

about any balance under the condition of bent rail. However, the minimum buckling strength does not represent the load that actually induces buckling.

In order to make clear the relation between the minimum buckling strength and the load that actually induces buckling, 400 model tests were carried out on tangent and curved tracks. The loads that induced buckling in the tests were found to be distributed in an approximately normalized form where theoretically calculated minimum buckling strength constituted a lower limit. Here, the relationship between longitudinal force at the time of buckling and lateral displacement of track panel is in agreement with the theoretical calculations. The variation of the loads that induced buckling was caused by track irregularity, variation of lateral ballast resistance, and the like. Furthermore, the results of buckling tests on full-scale track in 1957 demonstrated the theory's validity.

As stated above, Equation 1 gives the lowest magnitude of loads that induce buckling and has a certain margin to the longitudinal force that causes an actual buckling. The margin depends on the variation of ballast resistance, uneven lift of track panel, initial irregularity, and other factors. Thus, in practical application of Equation 1, 70 percent of measured ballast resistance is adopted, considering the variation of ballast resistance, uneven lift of track panel, and so on. Buckling stability also is examined, allowing for a margin of 20 percent for the longitudinal rail force determined by Equation 1. Thus a sufficient safety factor can be guaranteed. Because the equation is a little complicated, the following simplified equation, which yields a good approximate value, is preferred:
when $R \geq R_0$,

$$P_{t2}^* = 3.63\, J^{0.383} g^{0.535} N_j^{0.267} \tag{2}$$

when $R < R_0$,

$$P_{t1}^* = 3.81\, J^{0.383} g^{0.535} N_j^{0.267} - 20.2\, j^{0.789} N_j^{0.600}/R \tag{3}$$

where

R_0 = $(112.2\, J^{0.406} N_j^{0.333})/g^{0.535}$,
P_{tn} = track buckling strength (tf) expressed by the buckling waveform with the number of waves (n),
J = lateral rigidity,
g = lateral ballast resistance (kgf/cm),
r = longitudinal ballast resistance (kgf/cm),
N_j = flexural rigidity of track panel (including lateral rail rigidity and multiples of it), and
R = radius of curvature (m).

Buckling Analysis Using Energy Method

Thereafter, in order to give a theoretical basis to the actual buckling generating load, a theoretical analysis using an energy method was carried out (*2*). It is summarized as follows:

- As track deformation caused by buckling occurs, the first and second waveforms in Figure 1 are assumed.
- Lateral track resistance force (g) is expressed in Figure 5 as follows:

$$g = g_0 y/(y + a) \tag{4}$$

- Longitudinal ballast resistance is constant regardless of displacement.
- The rotating resistance moment is expressed by the formula

$$\tau = \tau_0 (\theta)^{1/2} \tag{5}$$

where τ_0 is a constant and θ is the angle of rotation.

- Longitudinal rail force after buckling is shown in Figure 6.

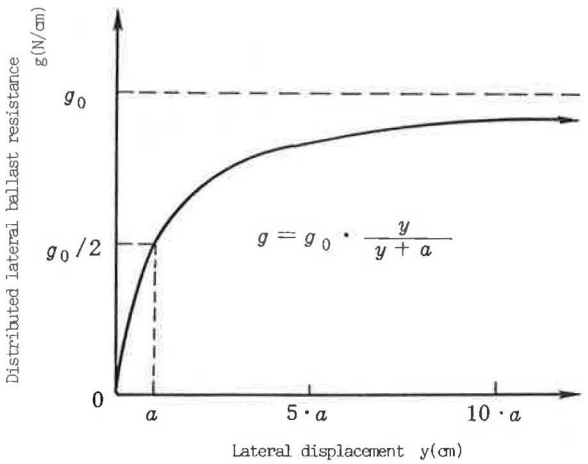

FIGURE 5 Characteristics of lateral ballast resistance.

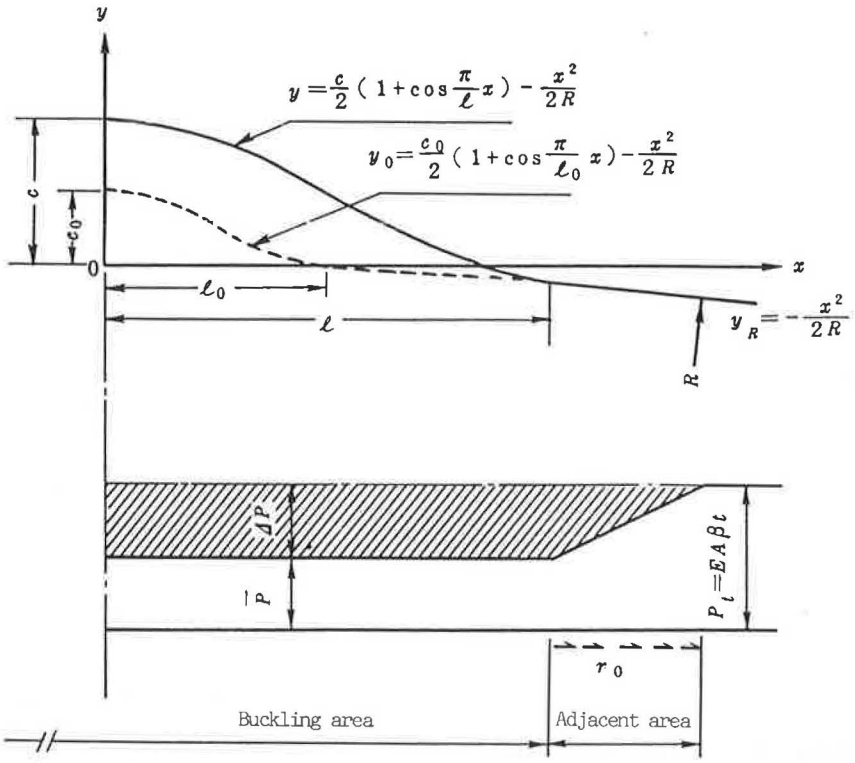

FIGURE 6 Assumption of deformation form and longitudinal force distribution (first waveform).

By virtue of the above, rail-axial strain energy, rail-bend strain energy accumulated in rail, work done against lateral and longitudinal ballast resistance, and work done to overcome the rotating resistance of rail fastening are determined.

When, on a track with initial irregularity, the total of the above-mentioned energies and of work done for track deformation wavelength (l) and lateral displacement (c) caused by a temperature rise (t) is equal to ΔU, this value has extremes depending on c and l, and the stability of deformation can be judged by these extremes. By fixing the lateral displacement magnitude c and partially differentiating with l, the minimum value of ΔU can be determined. The relationship between these ΔU and c is shown in Figure 7. A portion of the diagram with small values of c is on a linear scale, whereas the rest of the diagram with larger values of c is on a logarithmic scale.

The minimum value of ΔU indicates a stable balance, and the maximum value represents an unstable balance. Figure 7 shows that, when t is less than 40°C, the balance is stable only against minute displacements; when t is equal to 49°C, separate inflection points come out between C = 10 cm and C = 20 cm; when the temperature is higher than 49°C, a distinct minimum value appears within a larger displacement range. In other words, a stable balance generates in this range. When the temperature rises, the minimum value, or balance, can no longer be found in a minute displacement range—it exists only within a larger displacement range. The relationship between this minimum value and temperature variation t is shown in Figure 8, in which continuous lines indicate stable balance, and broken lines represent unstable balance.

Figure 8 shows that with less variation of temperature, a stable balance appears only under a minute deformation, whereas at a temperature exceeding a certain degree a stable balance emerges under a larger deformation as well as under a minute deformation. The longitudinal rail forces corresponding to the temperature variations coincide with the minimum buckling strength as described above. It is seen also from Figure 8 that, even with the temperature variation that exceeds the one corresponding to the minimum buckling strength, a balance state under a minimum deformation exists and does not immediately lead to a larger deformation.

The results of these analyses are as follows:

- An ultimate lateral ballast resistance considerably influences the maximum longitudinal force (Load A), under which a stable balance can be kept under a minute deformation and the minimum buckling strength (Load C).
- Initial characteristics of a lateral ballast resistance greatly influence Load A.
- A longitudinal ballast resistance has a great effect on Load C, but a small one on Load A.
- Influences of rotating resistance generated from rail fastenings are small in general.
- Alignment and inital track irregularity greatly influence Load A, but slightly influence Load C.

TESTS OF LATERAL TRACK STABILITY

Characteristics of Lateral Ballast Resistance

The characteristics of lateral ballast resistance have a great influence on buckling strength of track. Therefore, in order

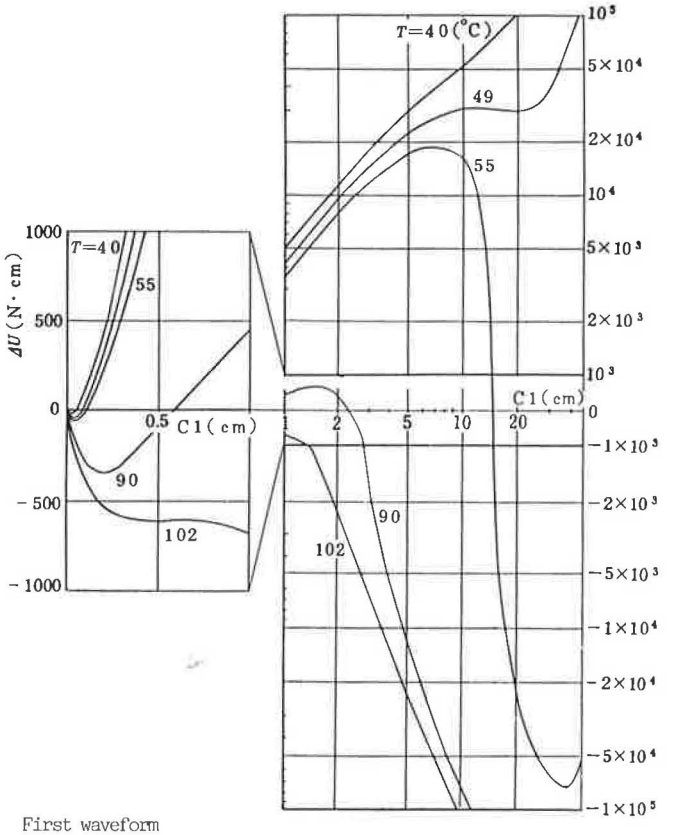

First waveform
R= ∞
50N Type rail (50.4kg/m)
Ultimate lateral ballast resistance form go=40N/cm
Initial characteristic coefficient of lateral ballast resistance a=0.1cm
Longitudinal ballast resistance ro=60N/cm
Rotating resistance moment of rail fastening device ro=5000N
Initial irregularity of alignment Maximum irregularity Co=2cm
Irregularity wavelength 2lo=10cm

FIGURE 7 Relation between energy variation and lateral displacement.

to evaluate lateral track stability, it is important to define the characteristics of ballast resistance. Lateral ballast resistance depends not only on dimension, geometry, mass, and spacing of ties but also on profile, bulk density, compacting magnitude of ballast, and so on. Figure 9 shows the characteristics of lateral ballast resistance that resulted from the tests with ties laterally pulled on the track under commercial operation. These tests have revealed that the characteristics of lateral ballast resistance are expressed by a hyperbola with a good approximation; lowered ballast resistance by tamping is restored in due course by train running; and so forth. In the meantime, as a result of the tests with ties laterally pulled on a test track, it has been ascertained that the lateral ballast resistance per tie is expressed by the following equation:

$$F = aW + brG_e + crG_s \tag{6}$$

where

F = ballast resistance per tie,
W = track mass on a tie,
r = bulk density of ballast,
G_e = statical moment of area around top chord of a tie end,
G_s = statical moment of area around top chord of tie side face, and
a, b, c = coefficients in Table 1.

Moreover, these tests have revealed that the tie bottom, side, and end surfaces share a third of the resistance with one another.

Buckling Tests

Several buckling tests, including the ones by Horikoshi as described above, were carried out on full-scale tracks in Japan.

The tests in 1932 were performed not only on a tangent track but also on curved tracks with radii of curvature 300 m and 500 m constructed on a 48-m-long test track. Longitudinal force was applied to the rail by means of hydraulic jacks and vapor pipe heating. The tests in 1956 were carried out on a 320-m-long test track with a 600-m curve radius. Longitudinal force was applied by vapor pipe heating, yielding data such as buckling wavelength and buckling length. In 1964, before the inauguration of the Shinkansen, on several sections of its line under varied ballast conditions, the rails were heated to buckling in trials with acetylene gas burners, verifying their safety against buckling.

Thereafter, beginning in 1981, a new buckling testing unit was installed on a full-scale track at the Railway Technical Research Institute, and seven series of various tests were performed, along with a study on a buckling stability theory. A test using this unit is shown in Figure 10. On a test section approximately 60 m long, the tests on tangent sections, curved track with radii of 300 m or less, and turnouts can be conducted. As for rail heating, a temperature rise to 70°C can be generated within 60 min with a flow of direct current through the rail.

The tests performed until now using this testing unit are as follows: buckling tests on a tangent section and curved sections with radii of curvature less than 400 m, buckling tests on wooden tie track, buckling tests that take the effect of load on the track into consideration, tests on longitudinal force characteristics of turnouts, and buckling tests on two tracks with different gages laid side by side. As a result of these tests, it was made clear that the value of a buckling-generating load on normal tracks is between Load A and Load C, determined by the theoretical analysis discussed previously. However, it is necessary to continue the investigation into the quantitative relationship between various factors and the buckling-generating load. The results of tests on sharp curve sections and turnouts have been implemented in engineering practices.

PRACTICES IN TRACK BUCKLING STABILITY

Laying and Maintenance of CWR

For lateral track stability, the track conditions for laying CWR in Japan were established as follows:

- For the rail with a mass of 50 kg/m or more, the number of ties must be more than 38 per rail unit length of 25 m;

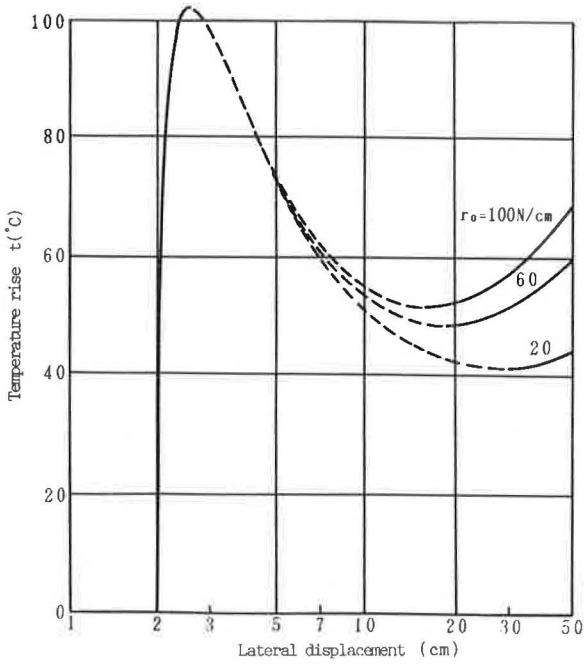

(A) Influence of Distributed Longitudinal Ballast Resistance (ro) (First waveform)

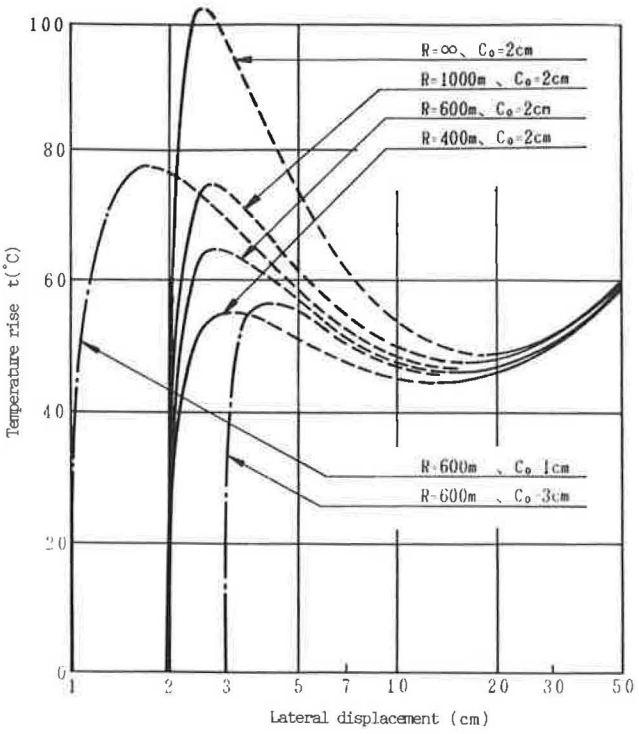

(B) Influence of Alignment and Initial Track Irregularity (First waveform)

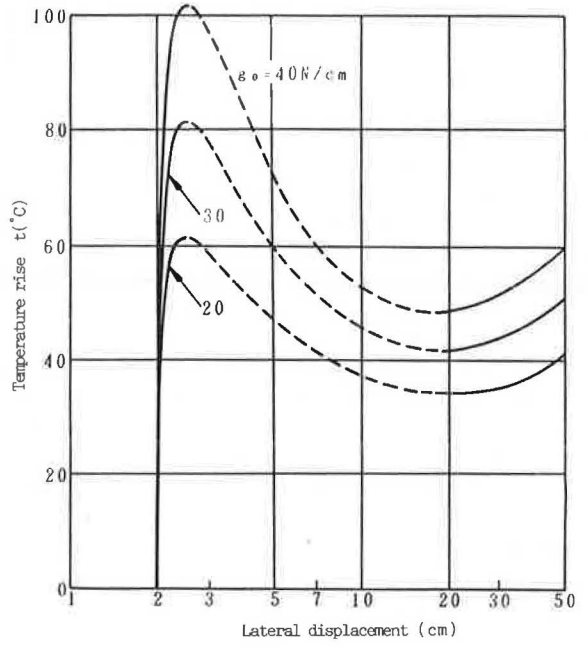

(C) Influence of Ultimate Distributed Lateral Ballast Resistance (go) (First waveform)

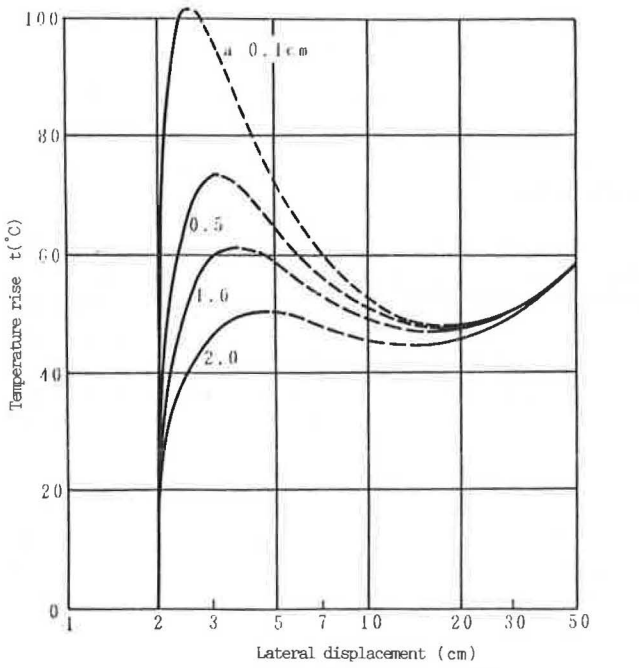

(D) Influence of Initial Characteristic (a) of Distributed Lateral Ballast Resistance (First waveform)

FIGURE 8 Relationship between temperature rise and lateral displacement.

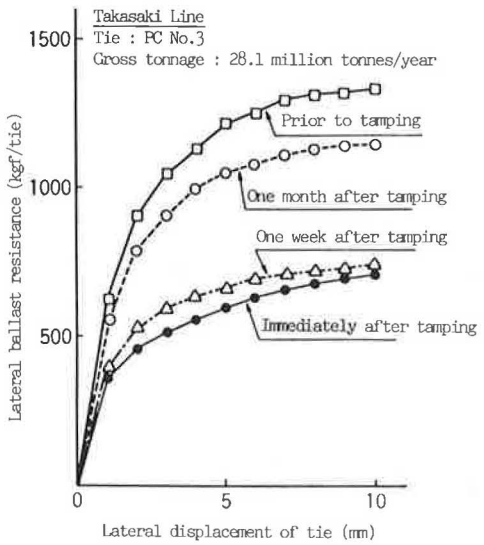

FIGURE 9 Characteristics of lateral ballast resistance.

TABLE 1 COEFFICIENTS FOR VARIOUS BALLASTS

Coefficients	a	b	c
Concrete tie and crushed stone ballast	0.75	29	1.8
Wooden tie and crushed stone ballast	0.75	29	1.3
Wooden tie and gravel ballast	0.6	29	1.4

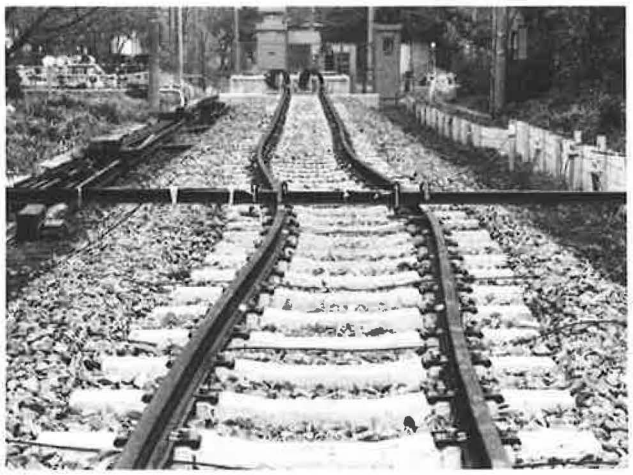

FIGURE 10 Full-scale test of track buckling.

- For track alignment, the radius of curvature must be 600 m or more, and the vertical curve radius at a changing point of gradient must be 2000 m or more;
- The road bed must be stable and free from subsidence;
- The ballast must consist of crushed stone;
- The ballast shoulder must be 400 mm or more wide;
- The lateral resistance must be kept to 4.0 N/mm or more for the 50-kg/m rail, and 5.0 N/mm or more for the 60-kg/m rail.

Meanwhile, on the Shinkansen lines that were constructed of CWR for high speeds of more than 200 km/h, it is specified that ballast resistance be more than 9.0 N/mm on the standard sections and more than 1000 kg/m on the sections subjected to additional force at bridge ends. Furthermore, the tightening temperature of CWR in general must be within the range shown in Figure 11.

A routine control of CWR track to prevent buckling is carried out such that its tightening temperature, creepage, work history at low temperature, and ballast conditions are grasped, which enables comprehensive decision making about the buckling stability of the track before the planning and implementation of CWR tightening changes, ballast maintenance, and so on. A flow chart depicting this process is shown in Figure 12.

To be more precise, when the tightening temperature is less than specified, or when work on rail renewal or on loosening and tightening of rail fastenings on a considerably long section is undertaken at a low temperature, or when creepages are different in different portions of a certain CWR, longitudinal rail force in the summer is greater than that of the standard CWR. A reduced additional temperature is determined by converting this additional longitudinal force into temperature difference, whereas a ratio of ballast resistance for the standard state is obtained from sectional geometry of ballast, which yields a safety factor through the following equation:

$$\alpha = 1.2i^{0.535}/(1 + \Delta t/\Delta t_{max}) \tag{7}$$

where

α = safety factor of CWR,
i = ratio of lateral ballast resistance,
Δt = reduced additional temperature, and
Δt_{max} = regularly allowable rate-of-rise from a tightening temperature.

The safety factor defined by the above equation is the ratio of the minimum buckling strength described previously to the maximum longitudinal rail force, including added longitudinal force. Depending upon this value, the necessity of tightening changes or ballast maintenance is decided.

Joint Gap Control on Jointed Track

The joint gap on jointed track must be maintained through periodic inspection, judgment, and alignment to ensure lateral track stability.

The judging standards for lateral track stability of rail joint gaps are categorized administratively in three ranks, according to the ratio of the maximum longitudinal force (P) on jointed track to the minimum buckling load (P_t) described previously. Here, the maximum longitudinal force (P) on jointed track is determined by the following equation:

$$P = EA\beta\,(t_{max} - t - e/\beta l) + R_0 \tag{8}$$

where

P = possible maximum longitudinal force,
E = Young's modulus for rail steel,

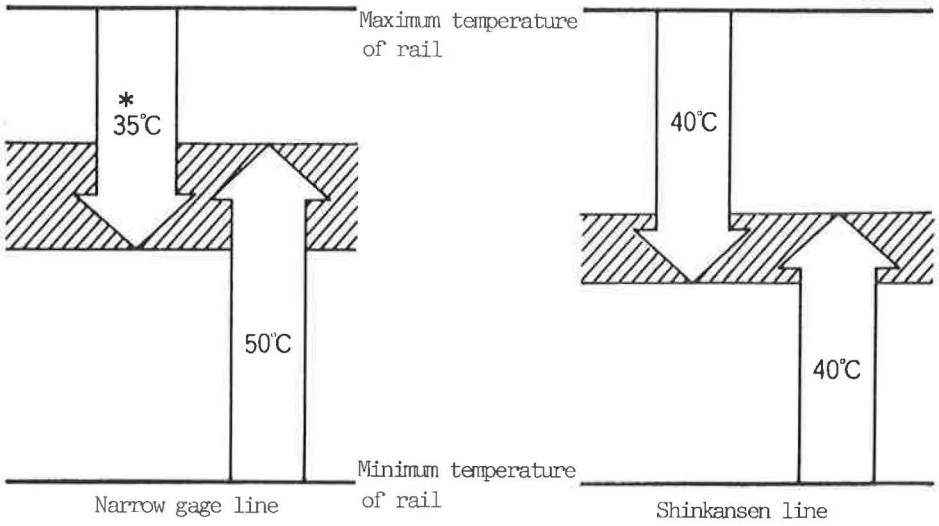

FIGURE 11 Tightening temperature of CWR.

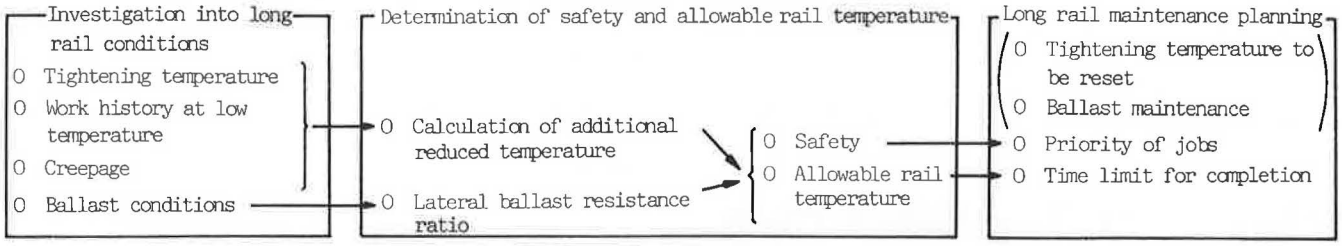

FIGURE 12 Concept of CWR maintenance.

β = coefficient of linear expansion for steel,
t_{max} = possible maximum rail temperature,
t = rail temperature at inspection,
e = rail joint gap at inspection,
l = rail length, and
R_0 = restraining force of joint bar.

RECENT STUDIES

CWR Use on Sharp Curves

CWR use in Japan so far has been limited to curve sections in which the radii of curvature exceed 600 m. The reason is that the volume of railway traffic in Japan is enormous and the frequency of rail renewal because of wear is high on sharp curve sections; the size of ties on the narrow gage lines is so small that the lateral ballast resistance is not sufficiently maintained, which leads to a lower safety against buckling. However, in order to fully exploit excellent features of CWR, it recently has been considered necessary to extend its use to curve sections in which the radii of curvature are smaller than 600 m. The study for implementing this idea is currently being undertaken.

According to the conventional theoretical analysis described previously, the effect of the radius of curvature on the minimum buckling strength is insignificant. Consequently, so long as buckling stability is evaluated in terms of the minimum buckling strength as in recent practice, CWR use on sharp curves should offer no serious problem. However, in practice, when safety on a sharp curve section is evaluated by means of the conventional method, it is feared that the real safety factor is lowered. Therefore, on the basis of the recent track buckling theory an investigation into its quantitative evaluation is being made.

Figure 7, expressing the variation of energy and workload induced by lateral track deformation, gives useful information pertaining to this problem. According to this figure, under a temperature variation of 49°C, which approximately corresponds to the minimum buckling strength (Load C), the value of ΔU corresponding to the balance state at major deformation (C = 20 cm) is at a higher level than the ΔU value at minor deformation (C = 0.1 cm or less). Here, in order to keep a balance state at major deformation, it is necessary to supply energy from the outside or to do work equivalent to the difference between these two ΔU values. Accordingly, it is likely that the difference in ΔU values between the two balance states has something to do with suppressing the buck-

ling. Thus, the relationship between ΔU values and radii of curvature is shown in Figure 13. It is evident from the figure that these values are considerably variable, depending on radii of curvature. From this fact, it seems that the minimum buckling strength does not much depend on the radius of curvature, while the margin to buckling is substantially lowered as the radius of curvature decreases. The quantitative relationship between ΔU value difference and safety factor to buckling as well as the relationship of ΔU values versus various factors lowering the buckling load on real track and their compensation must be investigated further.

CWR Connected to Turnouts

The connection of CWR to turnouts was tried early on the German Federal Railways (*3*). In Japan such an attempt was not made until recently except in experimental cases. Instead, expansion joints usually were located in front of and behind a turnout. One of the problems of direct connection of a turnout to CWR by welding or glueing is the increased longitudinal force generated near the point of the turnout by the two tracks being joined there.

In order to solve this problem, full-scale tests were carried out, complemented by a theoretical analysis (*4*). The outline is as follows:

- The model of a turnout track used is one shown in Figure 14.

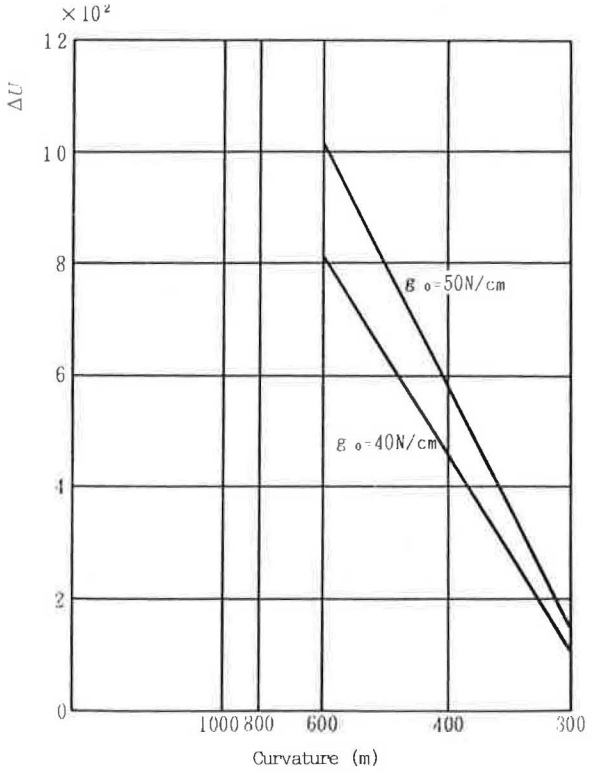

FIGURE 13 ΔU as a function of radius of curvature.

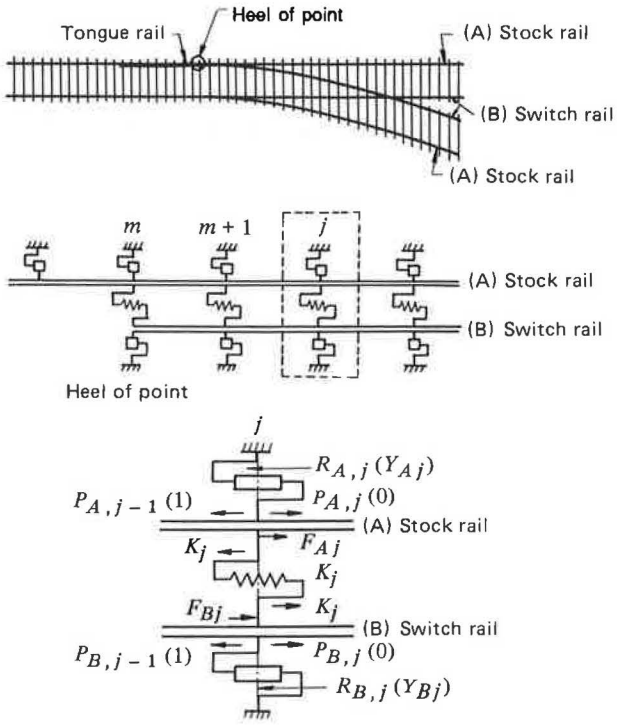

FIGURE 14 Dynamic model of turnout.

- Provided stock rail and lead rail are connected to each other through a spring system, the spring constant used is one obtained from full-scale tests.
- Characteristics of longitudinal ballast resistance are similar to the ones in Figure 5.

Under the conditions mentioned above, a computer simulation of the change of rail expansion and longitudinal force caused by temperature change was done. A comparison of the simulation results with measurements is made in Figure 15, which shows that the longitudinal rail force changes near the turnout, with its maximum value generated within the stock rail near the heel. The maximum value of the longitudinal rail force for the turnout rail is larger than that for standard CWR. Figure 16 shows the rate of longitudinal rail force increasing with parameters such as longitudinal ballast resistance and rail restraining spring constant. Comparison between the results of the above-mentioned analysis and full-scale tests has revealed the following:

- The results of analysis of longitudinal rail force agree well with analytical results of the full-scale tests.
- The maximum value of longitudinal rail force near the turnout generates near the heel portion of the turnout. The value is about 1.35 times the value of rail axial force in standard CWR.
- The restrained spring constant between rails and longitudinal ballast resistance influences the distribution of longitudinal rail forces but influences slightly its maximum value.
- Within about 30 m of the heel, longitudinal rail force is larger by 5 percent or more than the longitudinal force in

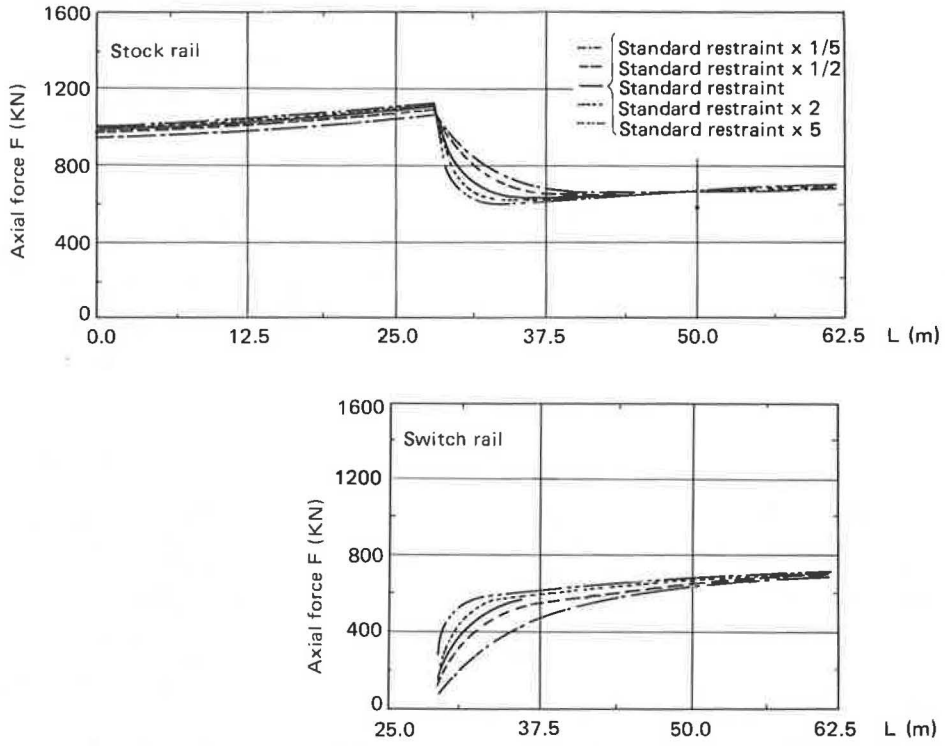

(A) Calculation

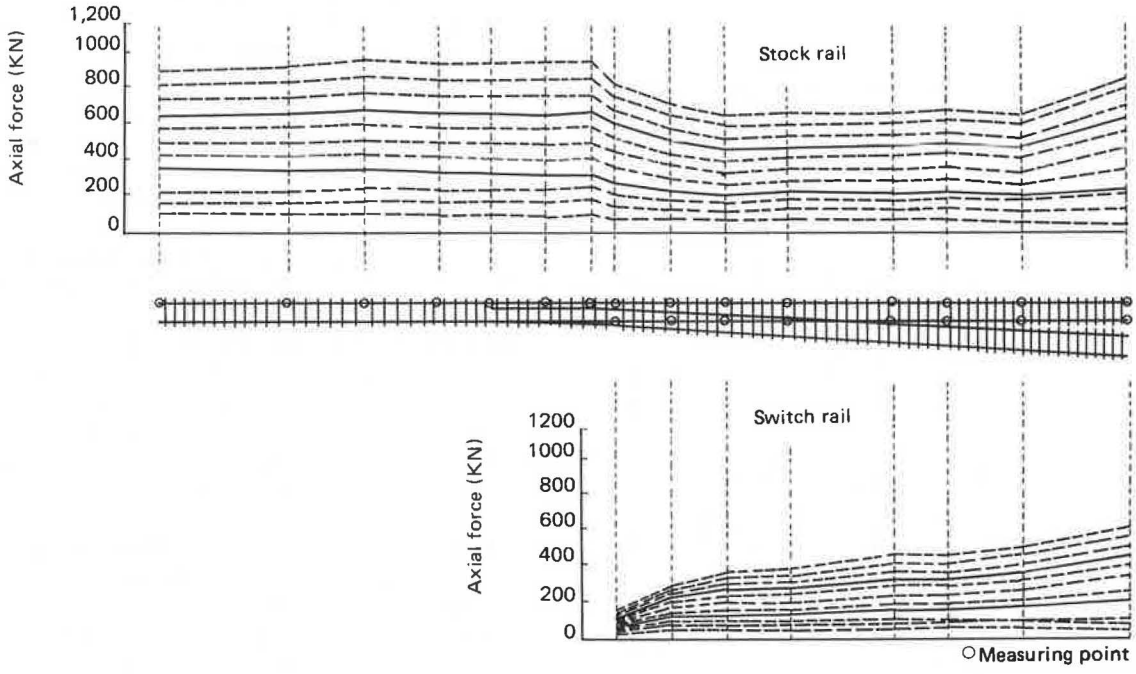

(B) Full Scale Test

FIGURE 15 Longitudinal force distribution of turnout.

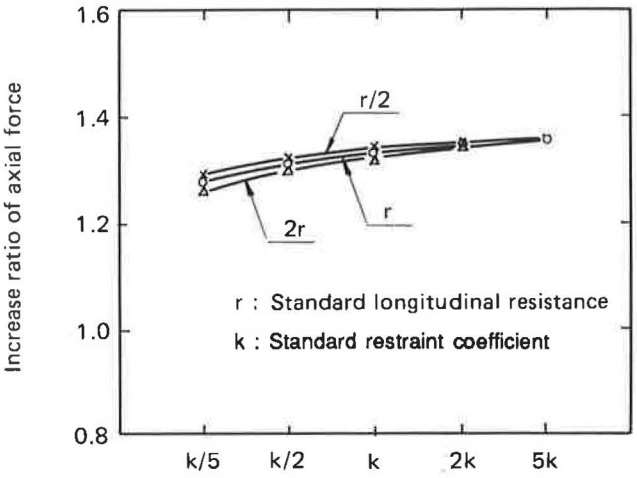

FIGURE 16 Variation of the maximum longitudinal force depending on *k* and *r*.

standard CWR under the same temperature variation as in the turnout rail.

- There is relative displacement between the stock rail and the point rail.

Owing to the above facts, when CWR is connected with the turnout, measures to increase ballast resistance at the 20- to 30-m-long portion of the turnout from the heel to the tip of the point rail should be taken. In addition, a means to prevent a large relative displacement between the stock rail and the point rail will be adopted. On this line, applications of CWR connected with turnouts are now advancing to the practical stage.

CONCLUSIONS

In Japan all the lines of the JR Group and most of the lines of private railways except for the Shinkansen with standard-gage track and some of private railways are on the 1067-mm-gage tracks. This gage has many disadvantages with respect to lateral track stability. It is difficult for this gage to hold sufficient lateral stability because the size of the ties and the mass of the ballast are smaller than those for the standard gage. Moreover, Japanese topography features mountainous terrain and hence many steep curves and gradients along the railway lines. Nevertheless, the railway traffic volume in Japan is considerably higher in comparison with foreign railways. Also, most of the traffic is generated from passenger operation. Consequently, it is very important to keep the track in good condition and to secure its lateral stability. It is believed that efforts so far and maintenance practices established on the basis of the results have been considerably successful, but the efforts are expected to be continued to make further advances.

REFERENCES

1. M. Numata. Buckling Strength of Continuous Welded Rail. *Bulletin, International Railway Congress Association*, 1960, pp. 33–49.
2. T. Miyai. Numerical Analysis of Track Buckling by Energy Methods. *Quarterly Report of RTRI*, Vol. 26, No. 3, 1985, pp. 81–84.
3. J. Eisenmann. Theory and Practice of the Continuous Welded Rail. *Railway Technical Review*, No. 27, 1985/86, pp. 35–39.
4. S. Miura and H. Yanagawa. Characteristics of Axial Force in Rail at Turnout Integrated with Continuous Welded Rail. *Quarterly Report of RTRI*, Vol. 30, No. 4, 1989, pp. 202–206.